



# Design and Control of Transfemoral Prosthesis Prototype with Magneto-Rheological Damper

Delond Angelo Jimenez-Nixon, Eng.<sup>1</sup>, Isaac Alejandro Venegas Lara, Eng.<sup>2</sup>, Joseb Josué Santamaria Rodríguez, Eng.<sup>3</sup>, Jose Marcelo Vega Rodriguez, Eng.<sup>4</sup>, Maria Celeste Paredes-Sanchez, Eng.<sup>5</sup>, and Alicia María Reyes-Duke, MSc. <sup>6</sup>

<sup>1,2,3,4,5,6</sup> Faculty of Engineering, Universidad Tecnológica Centroamericana (UNITEC), Honduras.

<sup>1</sup>[delondjimenez8@unitec.edu](mailto:delondjimenez8@unitec.edu), <sup>2</sup>[issac\\_venegas@unitec.edu](mailto:issac_venegas@unitec.edu), <sup>3</sup>[josebsantamaria@unitec.edu](mailto:josebsantamaria@unitec.edu), <sup>4</sup>[jmvr\\_1997@unitec.edu](mailto:jmvr_1997@unitec.edu),  
<sup>5</sup>[mariaceleste@unitec.edu](mailto:mariaceleste@unitec.edu), <sup>6</sup>[alicia.reyes@unitec.edu.hn](mailto:alicia.reyes@unitec.edu.hn).

*Abstract—This research aims to design, characterize, construct, and control a transfemoral prosthesis prototype with magneto-rheological damper to determine its functionality for aiding patients in Honduras. It was possible to design and control a transfemoral prosthesis prototype. Equally, the material (Aluminum) chosen, and the design that was presented meets the appropriate characteristics to resist a weight of an average person from Honduras of 80 kg, since a force of 400 N was applied in each of the parts.*

*Keywords—finite element analysis, prosthesis, control system, amputations, product design.*

**Digital Object Identifier:** (only for full papers, inserted by LACCEI).  
**ISSN, ISBN:** (to be inserted by LACCEI).  
**DO NOT REMOVE**

## I. INTRODUCTION

There is the possibility of being born without a lower or upper limb, or that this also arises through a surgical act. When facing a patient who requires an amputation, it is necessary to think not only about saving life but also about preserving good possibilities of independence and social reintegration. Lower limb prostheses only fulfill the function of replacing the limb and adding a tool to provide better support, which does not help to create a normal movement of the joints, nor do they present a type of cushioning that helps in impact against the ground, causing harm and discomfort; more pain in the stump that contacts the amputated area. A transfemoral prosthesis prototype with magnetorheological damper was designed, characterized, built and controlled for aiding patients in Honduras.

## II. THEORETICAL FRAMEWORK

### A. Anatomy of lower limb

The weight-bearing function of a lower limb makes the skeleton more massive and the joints more voluminous and stable, the muscle tissue is stronger, and the fascia is denser; This not only ensures segmental separation, but it also distributes muscle tension during the contraction process and helps support the effect[1]. Within the study of human anatomy, anatomical planes are the spatial references that serve to describe the arrangement of tissues, organs and systems and the relationships they have between them. They are practically three imaginary lines that cross the human body in different directions. It is necessary to place the origin in the center of mass of the body that is approximately in front of the second sacral vertebra, Fig.1 shows the relationship of the coordinate axes with respect to the anatomical planes [2].

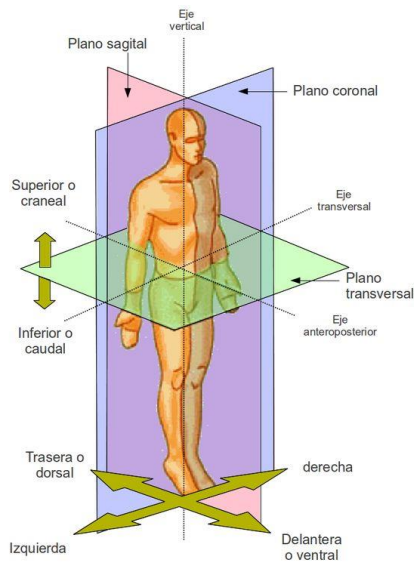


Fig. 1 Human body anatomic planes

### B. Lower limb amputations

According to [2] an amputation is considered a bone cut in healthy tissue or a part of the body in a joint. Amputation is required when an affected area in any part of the body is not expected to heal or when it is the product of different life occurrences such as accidents, cancer, circulatory disorders, among others. This forceful removal of limbs is aided by prostheses. Formally, a prosthesis is defined as a device of artificial nature aimed to substitute a lost limb due to an amputation or a genetic malformation, whose main function is to provide support, allowing walking and to cushion impacts, through the stability and correct alignment of the lower limbs, allowing the progression of the center of gravity. Moreover, the person will be able to carry out certain activities autonomously [3]. Fig. 2 presents the parts and components of a lower link prosthesis.

To carry out the design process for a lower limb prosthesis is of high importance to understand and analyze the gait cycle. This cycle describes the human being's walk, the moment in which the heel contacts the ground while the other foot is in the air. The stance phase has a percentage of 60% of the gait time and the balance phase with 40% to complete 100% [4].

The gait cycle is divided into two phases:

- The support phase
- The equilibrium phase



Fig. 2 Components of a lower link prosthesis.

### C. Damper

Shock absorbers have been very helpful over the years in lower limb prostheses. Due to their complex formation, they can absorb energy to reduce oscillations of some movement or also to reduce blows or impacts. One of the main topics of study in dampers is rheology. Rheology is of the study of the physical principles that regulate the movement of fluids. Its importance in metallurgy lies in the fact that one of the most typical operations is mining and extractive metallurgy, which consists of the movement of fluids, water, and pulp. During this activity an important parameter to control is viscosity. Viscosity depends on many parameters, in addition to obeying different

laws, depending on the material that is being produced. The viscosity of fluids depends mainly on temperature and to a lesser extent on pressure. The smaller the distance between the two surfaces the position tends to be linear, with the viscosity we can obtain the speed gradient that allows us to calculate the change in speed [5]. (1) and (2) show the formula for calculating the shear stress and dynamic viscosity of fluids.

$$\tau = \eta (\Delta y / \Delta v) \quad (1)$$

$$\eta = \tau (\Delta y / \Delta v) \quad (2)$$

Where:

$\tau$  = Represents shear stress.

$\eta$  = Represents dynamic viscosity of the fluid.

$\Delta y / \Delta v$  = Represents velocity gradient.

For the damper analysis, mathematical calculations will be required to determine the impact velocity, average velocity, absorption time, and impact force. These calculations are necessary because there is a difference in velocity and the height at which a person lifts his leg when walking. (3) allows for the calculation of the velocity of impact, (4) the average velocity, (5) damping time, and (6) impact force.

$$V_f = \sqrt{2 * h * g} \quad (3)$$

Where:

$V_f$  = Represents impact final velocity.

$h$  = Represents the height.

$g$  = Represents gravity.

$$V_m = (v_i + v_f) / 2 \quad (4)$$

Where:

$V_m$  = Represents average velocity.

$v_i$  = Represents initial velocity.

$v_f$  = Represents final velocity.

$$\Delta t = s / v_m \quad (5)$$

Where:

$\Delta t$  = Represents the difference in time to absorb the energy.

$s$  = Represents the displacement of the center of mass.

$v_m$  = Represents Average velocity.

$$F = ((m * v_f - m * v_i) / \Delta t) \quad (6)$$

Where:

$F$  = Represents the force.

$m$  = Represents the mass.

This study aims primarily to show the application of magnetorheological fluids. This type of fluid can respond in applications where magnetic fields are present changing their rheological behavior, the change mentioned is usually produced by a stress that grows with the magnetic field. Magnetorheological fluids are less well known than analogues.

By way of the application of external fields there is a polarization induced in the suspended particles resulting in the response of a MR (magnetorheological) fluid [6]. The particles that are in these chains have the task of restricting how the fluid moves fluid within the space because this increases the elastic limit of the fluid, then, the alteration of the attraction between the particles increases or decreases the strength of the field, allowing a control of the property's rheological fluid. Fig. 3 presents the graphic of the shear mode that the magnetorheological fluid is present in.

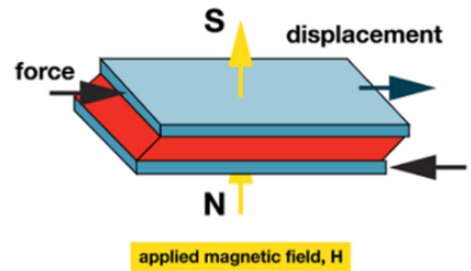


Fig. 3 MR fluid in shear mode

Finally, its necessary to induce the magnetorheological damper. Fig. 4 shows a typical MR damper and its piston assembly; this damper is a passive hydraulic type. The working principle of the MR damper is the conversion of shock into heat applying a fluid that moves through small holes in the piston between different chambers. A coil inside the piston creates a magnetic field when an electric current is supplied to the piston assembly. This magnetic field modifies the properties of the magnetorheological fluid instantly, causing the resistance of the damper to be continuously modified by modulating the electric current it receives in real time [7].

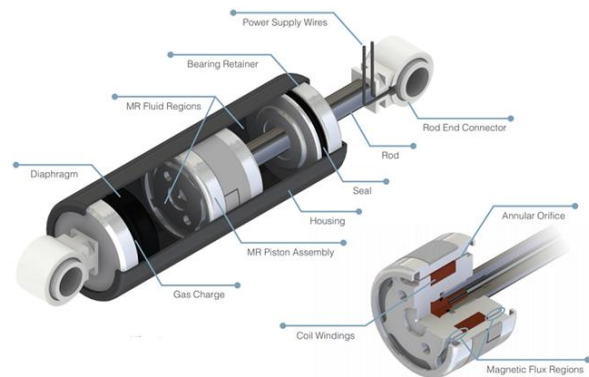


Fig. 4. A typical MR Damper and piston assembly

### III. STATE OF THE ART

Throughout the years there have been several studies and investigations in areas of magneto – rheological damper and transfemoral prosthesis. This literature review begins with a general overview of studies involving magneto rheological dampers. In 2021, Carabello et al. developed an investigation about orthopedic prosthetic sockets after transfemoral amputation by conducting a survey of ten orthopedic technicians with expertise in the field in Germany. The main findings show that the specialist paid very close attention to how the patient reacted during the fitting stage of the prosthesis, demonstrating the high levels of importance empathic interactions has on the overall experience of the user [8]. Gaoyu Liu et al. carry out a review article in [9] studying the progress of medical applications of MR fluids over a span of 20 years focusing mainly on 6 areas of interest covering from limb prosthesis to exoskeletons and rehabilitation devices, amongst others. The authors concluded that prostheses, exoskeletons, and limb orthoses with MR fluid perform movement with greater naturalness and stability. Muscle training with flexibility can be performed with rehabilitation devices and haptic feedback with high transparency and resolution. Oscar Arteaga et al. in 2018 presented a study [10] that analyzes the MR fluid MRF-140CG shining light on some of the main and primary properties it presents for its application in robotic prosthesis. Tests were performed with magnet field and dyno shock obtaining as a result a model of dynamic proportions. The results of comparison between different models aided in being able to have and design more efficient, intelligent, and sophisticated mechanical devices. Avila et al. in [11] use generative cad and fem analysis approaches in hand with additive manufacturing to offer a methodology for the transtibial prosthesis design. This development sets a standard for the current research of transfemoral prosthesis.

In areas of transfemoral prosthesis several studies have been carried out that add value to this current research. Dedic et al. [12] work on a leg prototype in the transfemoral category where work was done in regards to design from the concept to its optimization having obtained a CAD design ready for manufacturing process and learning a lot from simulations process and finite element analysis. Researchers from the School of Engineering at the University of Kerbala (Iraq) designed a controller for application in prosthesis under the above knee category that was mainly based on the intelligence and adaptability of the neurofuzzy system of inference. For the analysis done on the sagittal plane of the gait cycle, they used two strategies for collecting the data that are sent to the controller. The results of the research show that the ANFIS controllers had an excellent response when determining values of a knee joint such as moment and angle values which had an RMS error value of 0.006 [13]. In 2018, Fahad M Kadhim et al. designed and fabricated a microcontroller-based smart transfemoral prosthetic knee joint. This study aimed to improve the traditional high-cost passive prosthesis to a prosthesis that

could achieve a designated rotational speed during functional wear, which previous prosthesis were unable to reach. The main results of this study revealed the definition of the main materials used such as Aluminum Alloy 6061, AA 7075 and AISI 4130 Steel and the factors for this decision was discussed. Finally, the main characteristics of the final design were obtained via the finite element analysis [14].

In 2021, Kamel et al. [15] modelled and analyzed a prosthesis for use in amputations of transfemoral nature presenting a smart knee joint of novel proportions. The finite element method was applied where it's found that the displacement values and stress test are directly proportional to the flexion angle of the designed knee joint. Using a similar method, Sreya Reddy, Kesavapuram and M Dhanalakshmi [16] in 2022 carried out a study for amputations done above knee in order to designed a transfemoral prosthesis. The design replaced the pylon or the shank with a damper that allows for the knee joint to have mechanical characteristics that reduces the transient mechanical force by dispersing it evenly on the prosthesis. The design allows as the swing face occurs freedom of movement and flexion enabling the subject to jump and jog with ease. In terms of materials carbon fiber was selected over materials such as polyester resin and/or stainless steel. Thesleff et al. [17] studied loads during aided and free movement in transfemoral prosthesis that are osseointegrated. The loads are analyzed at the implant – prosthesis interface. This studies approach is aimed at quantifying how much load is applied during daily activities to a bone anchored type implant. It was concluded that for most participants, no activity can be considered as generating particularly high loads, even so, this study can be used to make individual recommendations on walking strategies and extension of walking aids.

An important precedent in transfemoral prosthesis development was the work done in 2011 by Lawson et al. in [18] where an improvement was done introducing a transfemoral prosthesis intelligently powered for standing stability, the controller used for this prosthesis is capable of estimating some important characteristics such as the ground slope within more or less  $1^\circ$  over a range from  $-15^\circ$  to  $+15^\circ$ , providing adequate impedance at the joint that gains importance when for standing on surface with slopes. During 2020, Pace et al. [19] optimized limb stability in a transfemoral prosthesis using a simple walking model. A pendulum singularly inverted is used as a base, the main purpose was to simulate the sagittal plane through a numerical model form limb stance, and it can be used to identify optimal solutions for foot stiffness on knee moment by predicting effects of prosthetic knee alignment. A simulation process is performed on single limb support for the prosthetic gait, such simulation underwent a validation process against gait data obtained in a lab setting. To complete this process a testbench is prepared, analyzed and synthesized to be able to test modules used in transfemoral prosthesis as well as control systems [20]. After reviewing all the important research

on magneto rheological dampers and transfemoral prostheses individually, its necessary to aid the development of the current study by reviewing developments where magneto rheological dampers included in transfemoral prostheses. During 2017, Chen et al. [21] keened on developments for exoskeletons for lower extremities where a characterization and design process was done for an MR actuator, which experimental results match the modeling and simulation. Results showed that during a gait cycle there was an improvement of 52.8% in terms of energy efficiency of the actuator compared with that of an electrical motor. Ma et al. [22] designed and tested a MR actuator with regenerative properties for knee braces used in assistance, there is a direct match and confirmation between simulation and modelling. According to results, the future is promising for RMRA developed assistive knee braces in applications such as assistance and rehabilitation. In 2020, further research was done on knee braces with controllability designing and characterizing an MR damper. It was concluded that during axial and bending tests, the device shows absorption capabilities up to 4.5 N and 0.39 displacement. These values are proportional to displacement allowance and current input for prosthesis. Automatic control of the magneto rheological elastomer devices can be carried out according to the results. [23]. In areas of optimization, optimization and control of the torque present in a MR knee prosthesis with active characteristics performed by Andrade et al. [24]. The objective was to use an algorithm in order to optimize the MR brake and/or clutch design in areas of geometry that way the volume, weight and energy consumption can see levels of reduction. To evaluate the design performance, a prototype was fabricated and tested using dynamic models to analyze the torque control, motor unit and braking system of the MR damper. From the results, it can be concluded that for applications that require low level in terms of energy consumption and weight, rapid response time intervals, size compactness and high active/braking torque, this MR damper offers very good performance. In 2017, research on smart knee prosthesis was done implement an MR damper equipped with optical characteristics was published by Gao et al. [25] aiming to reduce energy use levels during an individual gait cycle and the overall weight values of the damper. The total energy consumption was obtained by carrying out an analysis of all phases intergraded in a single gait cycle. Fu et al. [26] added a sliding mode used for tracking control purposes of a MR damper knee prosthesis design. Finally, in 2012 Mora et al. [27] performed a study for the compensation in terms of magnetorheology for transfemoral prosthesis controlling the prosthesis discretely to aid the human walking process. The analysis of the geometric place of roots was used for the design of the controller. Simulation on control systematics indicates the prosthesis can follow determined joint references accurately and reject external disturbances.

#### IV. METHODS

The approach chosen for the following investigation was quantitative, since it proves theories and tests are applied using

validation instruments, then it will be able to carry out the analysis of effort, movement, and resistance. The applied methodology for this research was the V methodology. It summarizes the main steps to be taken in conjunction with the corresponding deliverables of the validation systems, Fig. 5 presents the flow of the development carried out using this method.

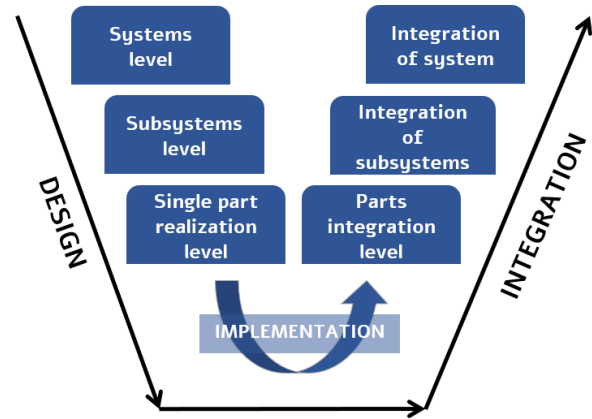


Fig. 5 V methodology used for the prototype designing.

#### V. RESULTS AND ANALYSIS

To develop the prototype of the transfemoral prosthesis, the systems were divided into three parts, the structural system, the control system, and the power system, and each one with its respective subsystem, Fig. 6.

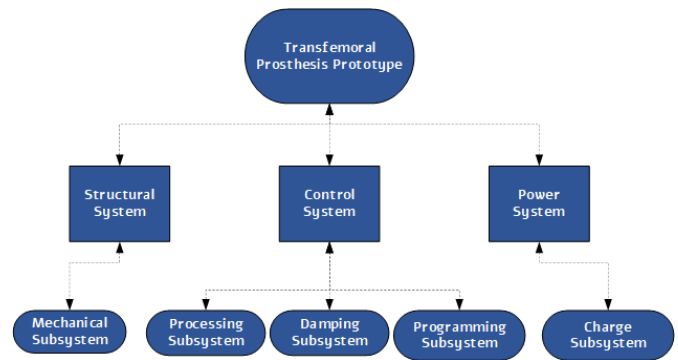


Fig. 6 Systems and subsystems diagram of the prototype

##### A. Mechanical subsystem

All the parts of the prototype were made in 3D SolidWorks, as well as simulation's tests to determine if the material could be adequate by predicting its performance under complex loads. The chosen material for the prosthesis structure was aluminum 5083; the foot was made of wood and the basin of polypropylene. To deduce how much mass the prototype would be supporting, Newton's second law (7) and (8) were considered based on the mass of the body parts.



$$F = m * a \quad (7)$$

$$w = m * g \quad (8)$$

Where  $F$  = total force that interacts with the body,  $m$  = mass of the body,  $a$  = acceleration,  $w$  = weight and  $g$  = gravity.

Within the calculations with (7) and (8), it was established that the nominal mass and height of a person for the simulation's tests would be 80 kg with 1.78 m. The weight exerted is approximately 390 N, so the parts developed in 3D SolidWorks were subjected to a weight of 400 N as shown in Fig. 7, 8, 9, 10.

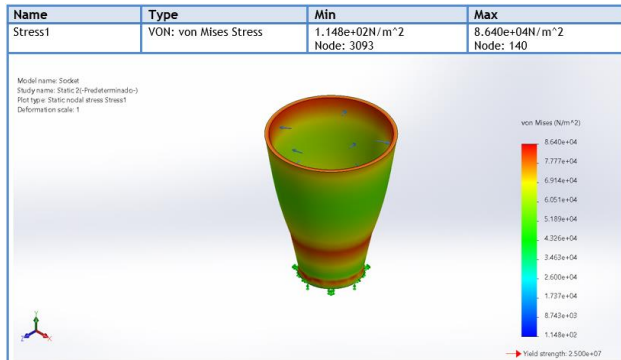


Fig. 7 Stress test performed for prosthesis basin.

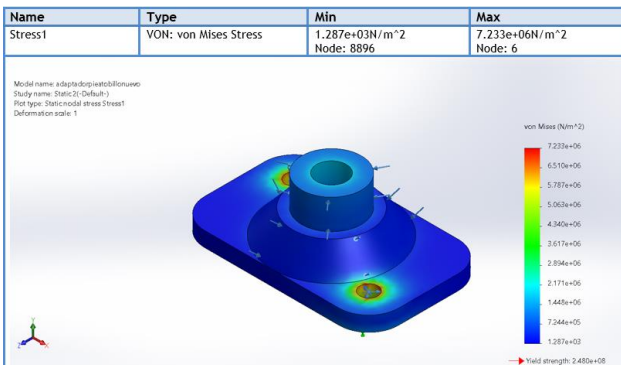


Fig. 8 Stress test performed for prosthesis upper link.

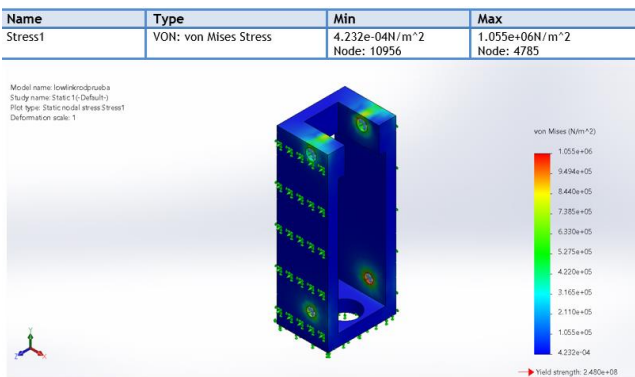


Fig. 9 Stress test performed for prosthesis base.

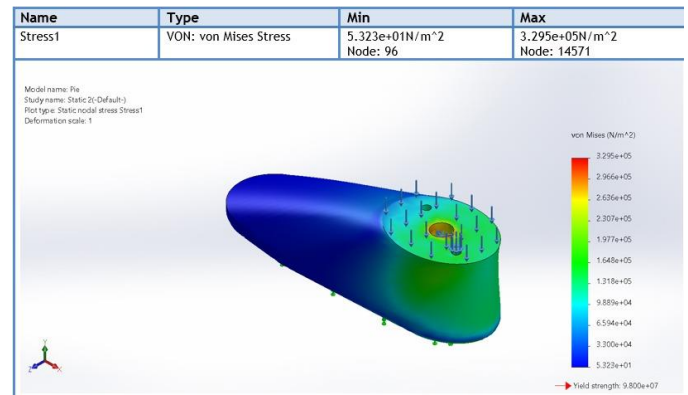


Fig. 10 Stress test performed for prosthesis wood foot.

The basin (Fig. 7) has a safety factor minimum of  $2.894e+02$  and maximum of  $2.178e+05$ . The upper connector is the part that connects the prosthesis structure to the basin. The stress test results show it has a minimum displacement of  $0.000e+00$  mm with a node of 77 and a maximum displacement of  $4.539e-04$  mm with a node of 335. As for the lower connector has a minimum stress result of  $1.287e+03$  N/m<sup>2</sup> with a node of 8.896 and maximum of  $7.233e+06$  N/m<sup>2</sup> with a node of 6. Its safety factor maximum is  $3.429e+01$  with a node of 6 and a minimum safety factor of  $1.927e+05$ . It has a minimum displacement of  $0.000e+00$  mm with a node of 1 and a maximum displacement of  $2.530e-04$  mm with a node of 12,229.

The upper link (Fig. 8) is connected with the magneto rheological damper and the upper connector, it is also the joints with the base structure. It has a minimum stress of  $1.807e+04$  N/m<sup>2</sup> with a node of 10,102 and maximum stress of  $4.588e+06$  N/m<sup>2</sup> with a node of 12,796. A displacement test was performed showing the results of minimum displacement  $0.000e+00$  mm with a node of 89 and maximum  $2.531e-04$  mm with a node of 86. The base (Fig. 9) has a minimum stress of  $4.232e+04$  N/m<sup>2</sup> with a node of 10.956 and maximum of  $1.055e+06$  N/m<sup>2</sup> with a node of 4.785. It has a minimum safety factor test of  $2.351e+02$  with node of 4.785 and maximum of  $5.860e+11$  with a node of 10.956.

The wood foot (Fig. 10) shows the minimum stress result of  $5.323e+01$  N/m<sup>2</sup> with a node of 96 and a maximum of  $3.295e+05$  N/m<sup>2</sup> with a node of 14.571 at the top. The factor of safety has a minimum result of  $2.974e+02$  with a node of 14.571 and maximum of  $1.841e+06$  with a node of 96. For the resulting displacement tests of the foot, the minimum result is  $0.000e+00$  mm with a node of 39 and the maximum displacement result is  $8.169e-04$  mm with a node of 191. The results of the foot show that it is capable of resisting a weight of 400 N, being the piece that resists the entire weight and is the one that is contacting the ground, it proves to be safe.

## B. Processing subsystem

A flow diagram was made to show the control and drive logic of the subsystem, Fig. 11. A battery energizes the

electronic components once these are connected to the power cable. The battery passes its power to a voltage and current regulator board that contains an ITC3780 microprocessor to perform this type of operation. The positive output of the board is connected to a common contact of a 5V relay that is powered by the Arduino nano development board that can deliver a voltage of 5V.

A relay is connected to a pin of the Arduino in which is activated or deactivated by a pulse from the digital output that functions according to the values that the MPU6050 gyroscope is reading. The values that are being detected and the parameters that were given defines if the normally open contact allows the flow of current and voltage that is connected to the common contact of the relay to pass through, thus allowing the damper to receive the amount of energy it needs. For a better visualization, some LEDs will indicate the status of the prosthesis, a green LED will be activated if the angle is greater than 15 degrees or a red LED when it is less than 15 degrees. There is also a voltage and current meter that is connected to the ITC3580.

common ground, Fig. 12. The Arduino is powered by the USB port of the computer.

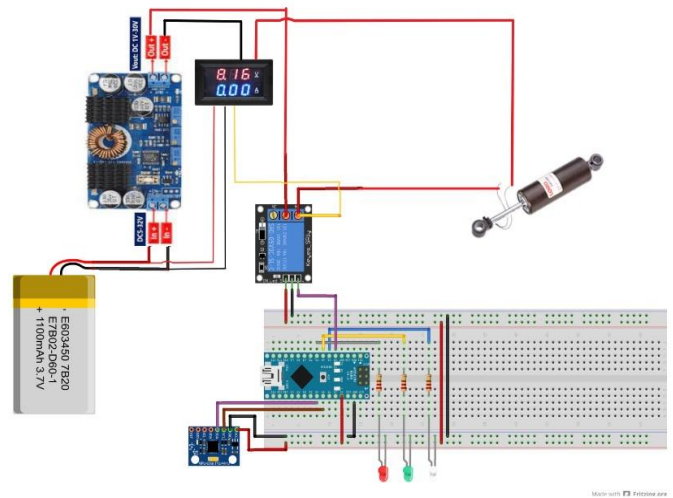


Fig. 12 Electronic circuit simulation in Fritzing

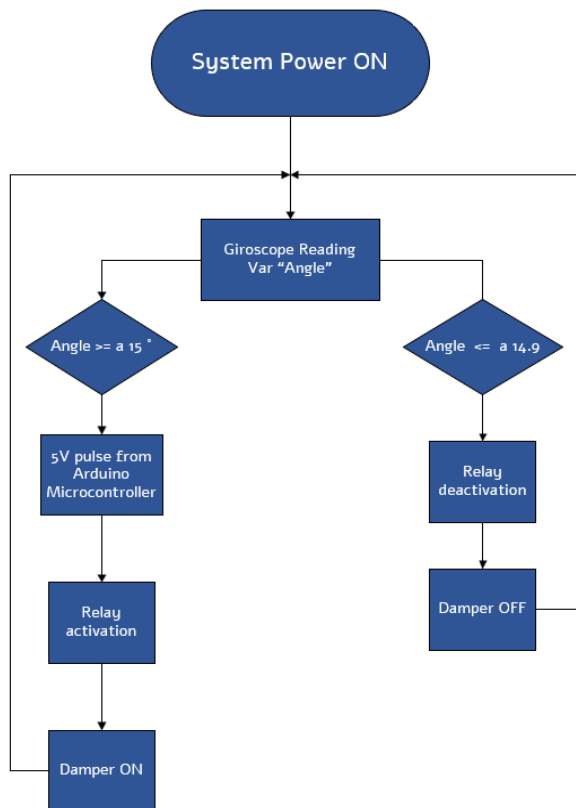


Fig. 11 Processing subsystem flow diagram.

### C. Damping subsystem

The LEDs and relay are connected in the digital pins of the Arduino board, meanwhile, in the analog inputs the gyroscope is connected, which is powered by the 5V supplied by the Arduino nano, where all the electronic devices must have a

A battery of 18 V was chosen. The ITC3780 board along with a voltage and current stabilizer, regulates the given input of the battery to deliver 12 V and 0.3 A to power the damper. The voltage and current meter are connected to the input of the stabilizer in which one of its wires is connected to the relay to measure the current; the next positive wire is connected to the negative port of the buffer and the negative of the voltage, and the current meter is connected to the negative output of the stabilizer and regulator.

(3), (4) (5), (6) were used to calculate the impact force that the individual has against the ground, considering a mass of 80 kg. In Table I, Calculations of various heights of the elevation made by the foot were made until returning to the ground in a range of 0.05 m to 0.125 m, since it is considered different types of walking. The displacement data of 0.05 m is already one of the characteristics of the damper by LORD company.

TABLE I  
IMPACT FORCE

Height	Final speed (m / s)	Average speed (m / s)	Damping time (s)	Impact force on one leg (N)
0.05 m	0.98	0.49	0.10	392
0.075 m	1.21	0.607	0.08	605
0.100 m	1.401	0.700	0.07	784
0.125 m	1.56	0.78	0.06	981

### D. Programming subsystem

Programming was done with the Arduino Software (a small fragment of the code is shown in Fig. 13), where tests and

library downloads were performed with the help of electronic components to allow the activation of the magneto-rheological damper.

```
// Include Wire Library for I2C
#include <Wire.h>

// Include NewLiquidCrystal Library for I2C
#include <LiquidCrystal_I2C.h>

// Define I2C Address - change if required
LiquidCrystal_I2C lcd(0x3F, 16, 2);

// Level LEDs
int levelLED_neg1 = 8;
int levelLED_neg0 = 9;
int levelLED_level = 10;
int levelLED_pos0 = 11;
int levelLED_pos1 = 12;
int rele=2;

//Variables for Gyroscope
int gyro_x, gyro_y, gyro_z;
long gyro_x_cal, gyro_y_cal, gyro_z_cal;
boolean set_gyro_angles;

long acc_x, acc_y, acc_z, acc_total_vector;
float angle_roll, acc_angle_pitch, acc;
```

Fig. 13 Programming fragment.

### E. Charge Subsystem

Using (9), it was calculated that the battery has 15 hours of autonomy. It was concluded the battery life duration is enough for long usages and since the battery is rechargeable it will not be a problem for the user.

$$H = (V_b * I_b) / (V_b * I_c) \quad (9)$$

Where  $H$  = hours of autonomy,  $V_b$  = battery voltage,  $I_b$  = battery intensity and  $I_c$  = current consumption.

### F. Prototype design

The mechanical parts of the prototype were assembled in SolidWorks as shown in Fig. 14. The designed prototype has a height of 61.09 cm, which agrees with the measurements of an average height of an adult in Honduras. In Fig. 15, it is possible to observe the constructed prototype assembled with its electronic and electrical components. It can be observed that when the basin is in vertical position, the red LED is on, which indicates that the basin is not at a sufficient angle for the voltage/current to pass through. When the blue and green LEDs are on, the blue one represents that the damper is on and the green one represents that there is an adequate inclination to activate the passage of voltage and current in the magneto-rheological damper, which is an angle greater than 15 degrees.

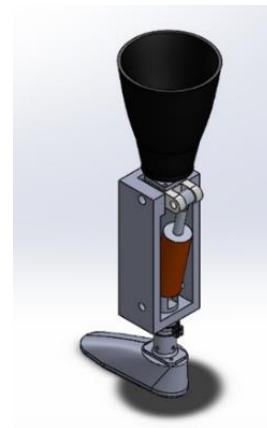


Fig. 14 Designed prototype in SolidWorks.



Fig. 15 Physical design of prototype.

## VI. CONCLUSIONS

It was verified that, through the selected components and devices, the project fully complies with the damping function, when it is greater than 15 degrees it is activated allowing the passage of voltage and current; if it is less than 14.9 degrees it will be deactivated. The circuit developed with the different electronic components manages to stabilize and regulate at the output a voltage of 12 V and a current of 0.3 A towards the damper. Through the final assembly the prototype can be adjustable to a minimum height of 66 cm and a maximum height of 69 cm. We can see that by means of 3D SolidWorks simulations, the material chosen and the design that was presented meets the appropriate measures to resist a weight of an average person from Honduras of 80 kg, since a force of 400 N was applied in each of the parts.

## VII. FUTURE WORK

For future work, it is recommended to add more sensors for better precision in the activation of the magneto rheological damper; make an electronic board to replace the electrical



circuit to reduce space for components and its function is more efficient; develop stress tests on the magneto rheological damper by means of special machinery to demonstrate the results based on frequency, amperage and applied force, and perform final walk tests on an individual.

## REFERENCES

- [1] M. Dufour, "Anatomía del miembro inferior," *EMC - Podol.*, vol. 14, no. 4, pp. 1–12, Nov. 2012, doi: 10.1016/S1762-827X(12)61929-4.
- [2] S. S. Salgado, "ALINEACIÓN EN PRÓTESIS DE MIEMBRO INFERIOR POR ENCIMA DE RODILLA," UNIVERSIDAD CES INGENIERÍA BIOMÉDICA ENVIGADO, Colombia, 2012. Accessed: May 02, 2023. [Online]. Available: [https://repository.eia.edu.co/bitstream/handle/11190/343/SalazarSara\\_2012\\_AlineacionProtesisMiembro.pdf?sequence=7&isAllowed=y](https://repository.eia.edu.co/bitstream/handle/11190/343/SalazarSara_2012_AlineacionProtesisMiembro.pdf?sequence=7&isAllowed=y)
- [3] A. Mota, "Materials of Prosthetic Limbs".
- [4] "Memorias del I Congreso Internacional de bioingeniería y sistemas inteligentes de rehabilitacion.pdf." Accessed: Feb. 06, 2023. [Online]. Available: <https://dspace.ups.edu.ec/bitstream/123456789/17080/1/Memorias%20del%20I%20Congreso%20Internacional%20de%20bioingenieria%20y%20sistemas%20inteligentes%20de%20rehabilitacion.pdf>
- [5] "Reología, la ciencia que estudia el movimiento de fluidos | Remetallica", Accessed: Feb. 06, 2023. [Online]. Available: <https://www.revistas.usach.cl/ojs/index.php/remetallica/article/view/1744>
- [6] L. A. G. Chavez and S. A. V. Duque, "Diseño y simulación de un sistema controlado de amortiguación para la rodilla de la prótesis transfemoral".
- [7] Parker, "How Does an MR Damper Work?" <https://www.parker.com/us/en/divisions/noise-vibration-and-harshness-division/solutions/semi-active-suspensions.html> (accessed Feb. 06, 2023).
- [8] A. Caraballo *et al.*, "Investigation of Orthopedic Prosthesis Socket Management after Transfemoral Amputation by Expert Survey," *Prosthesis*, vol. 3, no. 2, Art. no. 2, Jun. 2021, doi: 10.3390/prosthesis3020015.
- [9] G. Liu, F. Gao, D. Wang, and W.-H. Liao, "Medical applications of magnetorheological fluid: a systematic review," *Smart Mater. Struct.*, vol. 31, no. 4, p. 043002, Mar. 2022, doi: 10.1088/1361-665X/ac54e7.
- [10] O. Arteaga *et al.*, "Characterization of the magnetorheological fluid MRF-140 CG for applications in robotic prosthesis," *IOP Conf. Ser. Mater. Sci. Eng.*, vol. 522, p. 012006, Jun. 2019, doi: 10.1088/1757-899X/522/1/012006.
- [11] J. L. O. Avila, M. O. Avila, D. A. Aguilar, and M. Cardona, "Propose Method for the Design of a Transtibial Prosthesis using Generative CAD/FEM Analysis and Additive Manufacturing," in *2021 IEEE International Conference on Machine Learning and Applied Network Technologies (ICMLANT)*, Dec. 2021, pp. 1–7, doi: 10.1109/ICMLANT53170.2021.9690535.
- [12] R. Dedić, F. Ustamujić, Z. Jelačić, Ž. Husnić, and V. Kvesić, "Concept design and design optimization of the transfemoral prosthetic leg prototype," *IOP Conf. Ser. Mater. Sci. Eng.*, vol. 1208, no. 1, p. 012017, Nov. 2021, doi: 10.1088/1757-899X/1208/1/012017.
- [13] D. A. Kadhim, M. N. Raheema, and J. S. Hussein, "Design of an Intelligent Controller for Above Knee Prostheses based on an Adaptive Neuro-Fuzzy Inference System," *IOP Conf. Ser. Mater. Sci. Eng.*, vol. 671, no. 1, p. 012066, Jan. 2020, doi: 10.1088/1757-899X/671/1/012066.
- [14] F. M. Kadhim, J. S. Chiad, and A. M. Takhakh, "Design And Manufacturing Knee Joint for Smart Transfemoral Prosthetic," *IOP Conf. Ser. Mater. Sci. Eng.*, vol. 454, p. 012078, Dec. 2018, doi: 10.1088/1757-899X/454/1/012078.
- [15] S. H. Kamel, M. N. Hamzah, Q. A. Atiyah, and S. A. Abdulateef, "Modeling and Analysis of a Novel Smart Knee Joint Prosthesis for Transfemoral Amputation," *IOP Conf. Ser. Mater. Sci. Eng.*, vol. 1094, no. 1, p. 012109, Feb. 2021, doi: 10.1088/1757-899X/1094/1/012109.
- [16] S. R. Kesavapuram and M. Dhanalakshmi, "Design of transfemoral prosthesis for above the knee amputees," *J. Phys. Conf. Ser.*, vol. 2318, no. 1, p. 012032, Aug. 2022, doi: 10.1088/1742-6596/2318/1/012032.
- [17] A. Thesleff, E. Häggström, R. Tranberg, R. Zügner, A. Palmquist, and M. Ortiz-Catalan, "Loads at the Implant-Prosthesis Interface During Free and Aided Ambulation in Osseointegrated Transfemoral Prostheses," *IEEE Trans. Med. Robot. Bionics*, vol. 2, no. 3, pp. 497–505, Aug. 2020, doi: 10.1109/TMRB.2020.3002259.
- [18] B. E. Lawson, H. A. Varol, and M. Goldfarb, "Standing Stability Enhancement With an Intelligent Powered Transfemoral Prosthesis," *IEEE Trans. Biomed. Eng.*, vol. 58, no. 9, pp. 2617–2624, Sep. 2011, doi: 10.1109/TBME.2011.2160173.
- [19] A. Pace, D. Howard, S. A. Gard, and M. J. Major, "Using a Simple Walking Model to Optimize Transfemoral Prostheses for Prosthetic Limb Stability—A Preliminary Study," *IEEE Trans. Neural Syst. Rehabil. Eng.*, vol. 28, no. 12, pp. 3005–3012, Dec. 2020, doi: 10.1109/TNSRE.2020.3042626.
- [20] A. Poliakov, P. Gadkov, M. Kolesova, V. Lazarev, P. Bugayov, and P. Shtanko, "System analysis and synthesis of mechatronic testbench for testing modules and control systems of transfemoral prostheses," in *2015 8th Biomedical Engineering International Conference (BMEiCON)*, Nov. 2015, pp. 1–5, doi: 10.1109/BMEiCON.2015.7399555.
- [21] H. Ma, B. Chen, X. Zhao, H. Ma, L. Qin, and W.-H. Liao, "Design and characterization of a magneto-rheological series elastic actuator for a lower extremity exoskeleton," *Smart Mater. Struct.*, vol. 26, no. 10, p. 105008, Sep. 2017, doi: 10.1088/1361-665X/aa8343.
- [22] H. Ma, B. Chen, L. Qin, and W.-H. Liao, "Design and testing of a regenerative magnetorheological actuator for assistive knee braces," *Smart Mater. Struct.*, vol. 26, no. 3, p. 035013, Feb. 2017, doi: 10.1088/1361-665X/aa57c5.
- [23] N. H. Amer, K. Hudha, Z. A. Kadir, M. L. H. A. Rahman, and Mohd. S. Rahmat, "Design and Characterization of a Controllable Knee Braces with Magneto-Rheological Damper," in *2020 16th IEEE International Colloquium on Signal Processing & Its Applications (CSPA)*, Langkawi, Malaysia: IEEE, Feb. 2020, pp. 98–101, doi: 10.1109/CSPA48992.2020.9068671.
- [24] R. M. Andrade, A. B. Filho, C. B. S. Vimieiro, and M. Pinotti, "Optimal design and torque control of an active magnetorheological prosthetic knee," *Smart Mater. Struct.*, vol. 27, no. 10, p. 105031, Sep. 2018, doi: 10.1088/1361-665X/aadd5c.
- [25] F. Gao, Y.-N. Liu, and W.-H. Liao, "Optimal design of a magnetorheological damper used in smart prosthetic knees," *Smart Mater. Struct.*, vol. 26, no. 3, p. 035034, Feb. 2017, doi: 10.1088/1361-665X/aa5494.
- [26] Q. Fu, D.-H. Wang, L. Xu, and G. Yuan, "A magnetorheological damper-based prosthetic knee (MRPK) and sliding mode tracking control method for an MRPK-based lower limb prosthesis," *Smart Mater. Struct.*, vol. 26, no. 4, p. 045030, Mar. 2017, doi: 10.1088/1361-665X/aa61f1.
- [27] P. Zuly A Mora, S. M. Vásquez, C. H. Valencia, J. J. Carreño Zagarra, M. Becker, and P. A. Ospina Henao, "Discrete control of transfemoral prostheses for human walking with magnetorheological compensation," *J. Phys. Conf. Ser.*, vol. 2307, no. 1, p. 012017, Sep. 2022, doi: 10.1088/1742-6596/2307/1/012017.